Molecular mechanisms determining conserved properties of short-term synaptic depression revealed in NSF and SNAP-25 conditional mutants

Fumiko Kawasaki and Richard W. Ordway[1]

Department of Biology and Center for Molecular and Cellular Neuroscience, Pennsylvania State University, University Park, PA 16802

Communicated by Howard A. Nash, National Institutes of Health, Bethesda, MD, July 2, 2009 (received for review February 15, 2009)

Current models of synaptic vesicle trafficking implicate a core complex of proteins comprised of *N*-ethylmaleimide-sensitive factor (NSF), soluble NSF attachment proteins (SNAPs), and SNAREs in synaptic vesicle fusion and neurotransmitter release. Despite this progress, major challenges remain in establishing the in vivo functions of these proteins and their roles in determining the physiological properties of synapses. The present study employs glutamatergic adult neuromuscular synapses of *Drosophila*, which exhibit conserved properties of short-term synaptic plasticity with respect to mammalian glutamatergic synapses, to address these issues through genetic analysis. Our findings establish an in vivo role for SNAP-25 in synaptic vesicle priming, and support a zippering model of SNARE function in this process. Moreover, these studies define the contribution of SNAP-25-dependent vesicle priming to the detailed properties of short-term depression elicited by paired-pulse (PP) and train stimulation. In contrast, NSF is shown here not to be required for WT PP depression, but to be critical for maintaining neurotransmitter release during sustained stimulation. In keeping with this role, disruption of NSF function results in activity-dependent redistribution of the t-SNARE proteins, SYNTAXIN and SNAP-25, away from neurotransmitter release sites (active zones). These findings support a role for NSF in replenishing active zone t-SNAREs for subsequent vesicle priming, and provide new insight into the spatial organization of SNARE protein cycling during synaptic activity. Together, the results reported here establish in vivo contributions of SNAP-25 and NSF to synaptic vesicle trafficking and define molecular mechanisms determining conserved functional properties of short-term depression.

comatose | *Drosophila* | priming | SNARE | temperature-sensitive

A wide variety of synapses exhibit short-term synaptic depression in response to repetitive stimulation. Although the underlying mechanisms remain a matter of intensive study and debate (1), it is generally agreed that many forms of short-term depression include activity-dependent changes in neurotransmitter release. In some cases, depression has been attributed to depletion of release-ready synaptic vesicle pools (1–6), and in depth analysis of certain mammalian synapses has defined the physiological factors underlying and accompanying depletion (7–10). Such studies have established the detailed functional properties of short-term synaptic depression. To further investigate the molecular determinants of these properties, the present study combines genetic approaches with detailed electrophysiological analysis of short-term depression at adult neuromuscular synapses of *Drosophila*. This system permits conserved properties of short-term synaptic depression to be examined in temperature-sensitive (TS) paralytic mutants allowing acute perturbation of specific gene products at native synapses.

Studies of the neurotransmitter release apparatus have defined core protein interactions involving SNAREs of the synaptic vesicle membrane (v-SNAREs) and presynaptic plasma membrane (t-SNAREs), as well as *N*-ethylmaleimide-sensitive factor (NSF) and soluble NSF attachment proteins (SNAPs) (11, 12). Formation of SNARE complexes involves assembly of a four helix bundle composed of one SNARE helix from the v-SNARE, SYNAPTOBREVIN, one from the t-SNARE, SYNTAXIN, and two from the t-SNARE, SNAP-25. Current models suggest that synaptic vesicle priming involves partial assembly of "loose" SNARE complexes in a *trans* configuration between the synaptic vesicle and presynaptic plasma membranes. Subsequent full assembly ("zippering") of SNARE complexes in response to calcium influx may drive vesicle fusion (11, 13–15). After fusion, NSF and SNAP may disassemble *cis*-SNARE complexes in the plasma membrane.

Previous analysis of the *Drosophila* TS NSF mutant, *comatose* (16–18), demonstrated an in vivo role for NSF in synaptic transmission (19, 20), as well as disassembly of plasma membrane SNARE complexes (21). Studies of a TS SNAP-25 mutant, *SNAP-25^{TS}*, identified a missense mutation within the N-terminal half of the first SNARE helix, which disrupts specific aspects of SNAP-25 function (see ref. 22 and *Discussion*). The present study builds on previous analysis of synaptic transmission in *Drosophila* (23) by revealing conserved properties of short-term synaptic depression at adult neuromuscular synapses and employing these conditional mutants to examine the underlying molecular determinants.

Results

NSF and SNAP-25 TS Paralytic Mutants Exhibit a Conditional and Activity-Dependent Reduction in Neurotransmitter Release. Excitatory postsynaptic currents (EPSCs) were recorded at dorsal longitudinal flight muscle (DLM) neuromuscular synapses of the *Drosophila* adult. Under normal physiological conditions, WT synapses displayed mild short-term synaptic depression in response to 1-Hz train stimulation. At a restrictive temperature of 33 °C, both *comatose* (NSF) and *SNAP-25^{TS}* exhibited a WT EPSC in response to the first stimulus; however, subsequent stimulation in each mutant produced a marked activity-dependent reduction in EPSC amplitude relative to WT (Fig. 1). Rescue of the *comatose* (NSF) and *SNAP-25^{TS}* synaptic phenotypes was achieved by neural (presynaptic) expression of transgenes encoding WT forms of the *comatose* gene product, dNSF1 (17, 18, 24, 25) (Fig. 1*D*), and SNAP-25 (Fig. 1*E*), respectively. These findings indicate that both *comatose* (NSF) and *SNAP-25^{TS}* mutants exhibit an activity-dependent reduction in neurotransmitter release. The conditional nature of these synaptic phenotypes is discussed in *SI Methods* (see Fig. S1). Despite the activity-dependent reduction in EPSC amplitude observed in both mutants at 33 °C, the WT EPSC waveform was preserved throughout the stimulus train (Fig. 1 *F–I*). Thus, neither *comatose* (NSF) nor *SNAP-25^{TS}* disrupts WT kinetics of neurotransmitter exocytosis as determined by presynaptic calcium channel activation, coupling of calcium influx to synchronous synaptic vesicle fusion, and the membrane fusion mechanism permitting release of neurotransmitter. Rather, both mutants ap-

Author contributions: F.K. and R.W.O. designed research, performed research, analyzed data, and wrote the paper.

The authors declare no conflict of interest.

[1]To whom correspondence should be addressed. E-mail: rwo4@psu.edu.

This article contains supporting information online at www.pnas.org/cgi/content/full/0907144106/DCSupplemental.

www.pnas.org/cgi/doi/10.1073/pnas.0907144106

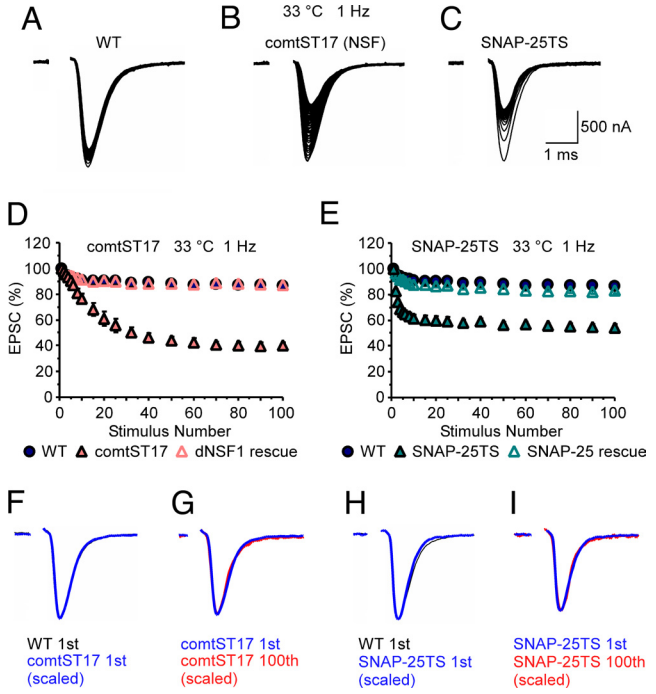

Fig. 1. The *comatose* (NSF) and *SNAP-25* TS paralytic mutants exhibit a conditional and strictly activity-dependent reduction in neurotransmitter release. (*A–C*) EPSC recordings at DLM neuromuscular synapses of WT (*A*), *comatose*^{ST17} [comST17 (NSF)] (*B*), and *SNAP-25*^{TS} (*C*) at 33 °C. Each panel shows superimposed current traces representing the first 100 responses. Stimulation artifacts were removed for clarity. Initial EPSC amplitudes at 33 °C in WT, *comatose*^{ST17}, and *SNAP-25*^{TS} were 2.01 ± 0.06 μA (n = 49), 1.99 ± .08 μA (n = 27), and 1.88 ± 0.05 μA (n = 33), respectively, and not significantly different from one another. (*D* and *E*) Peak EPSC amplitudes normalized to the initial amplitude are plotted as a function of stimulus number (n = 4–5). Here, and in subsequent figures, data points represent the mean ± SEM. The activity-dependent synaptic phenotypes observed in *comatose*^{ST17} (*D*) and *SNAP-25*^{TS} (*E*) were rescued by neural (presynaptic) expression of the corresponding WT proteins. Rescue of *comatose*^{ST17} was carried out in *Appl-GAL4 comatose*^{ST17}*;;UAS-dNSF1-FLAG/+* flies. Rescue of *SNAP-25*^{TS} was performed in *Appl-GAL4;;UAS-tdTomato-SNAP-25 SNAP-25*^{124}*/SNAP-25*^{TS} flies. (*F–I*) WT synaptic current wave form in both TS mutants. EPSCs were evoked by 1-Hz stimulation at 33 °C. The first EPSC in WT (black in *F* and *H*) was superimposed with a scaled version of the first EPSC in *comatose*^{ST17} (blue in *F*) or *SNAP-25*^{TS} (blue in *H*). Similarly, the first EPSC in *comatose*^{ST17} (blue in *G*) or *SNAP-25*^{TS} (blue in *I*) was superimposed with a scaled version of the respective 100th EPSC (red in *G* and *I*). No change in the EPSC waveform was observed in either mutant.

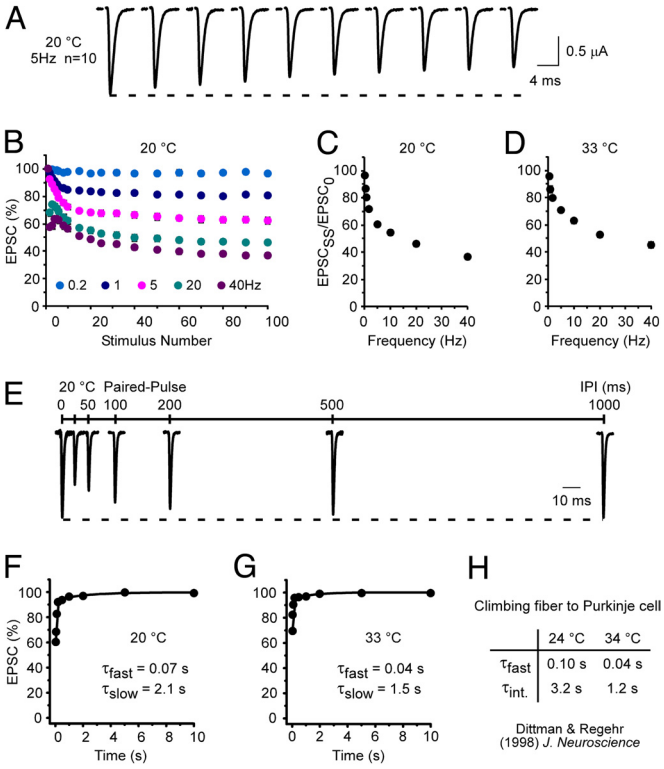

Fig. 2. Properties of short-term synaptic depression at WT adult DLM neuromuscular synapses. (*A–D*) Frequency dependence of short-term depression. (*A*) Example recording of the first 10 EPSCs evoked by 5-Hz stimulation at 20 °C. For display purposes, portions of the current trace corresponding to IPIs are not shown. (*B*) Peak EPSC amplitudes at 20 °C were normalized and plotted as a function of stimulus number over a range of stimulation frequencies (0.2–40 Hz) (n = 4–9). (*C* and *D*) Steady-state depression, expressed as the ratio of steady-state and initial EPSC amplitudes ($EPSC_{SS}/EPSC_0$), is plotted versus stimulation frequency at 20 °C (n = 4–9) (*C*) or 33 °C (n = 4–7) (*D*). (*E–H*) Two components of recovery in PPD. (*E*) Example EPSCs evoked by PP stimulation with IPIs of 25–1,000 ms at 20 °C. Pairs of EPSCs representing different IPIs were scaled relative to the first EPSC and superimposed. (*F* and *G*) The time course of recovery in PPD (n = 4–7) was fit with two exponential components (solid lines) exhibiting τ_{fast} = 0.07 s (89%) and τ_{slow} = 2.07 s (11%) at 20 °C (*F*), and τ_{fast} = 0.04 s (90%) and τ_{slow} = 1.46 s (10%) at 33 °C (*G*). (*H*) Corresponding recovery components in PPD at cerebellar CF-PC synapses (2).

pear to exhibit an activity-dependent reduction in the number of vesicles that fuse in response to an action potential. Despite the similarities in the synaptic phenotypes of *comatose* (NSF) and *SNAP-25*^{TS}, interesting and important differences were observed as well.

Conserved Properties of Short-Term Synaptic Depression at Adult DLM Neuromuscular Synapses. The preceding observations suggested that analysis of TS paralytic mutants may further define the in vivo contributions of NSF and SNAP-25 to the detailed properties of synaptic function. Thus, further electrophysiological characterization was undertaken in WT to establish the adult DLM neuromuscular synapse as a suitable model for these studies. At both 20 and 33 °C, frequencies >0.5 Hz produced a progressive decline in EPSC amplitude to a steady-state level (Fig. 2 *A–D*). Several properties of short-term depression were conserved with respect to other systems, including the relationship between steady-state depression and stimulation frequency (Fig. 2 *C* and *D*) (2, 5, 6, 26), and apparent facilitation in the initial stages of higher frequency trains (20 and 40 Hz) (Fig. 2*B*) (27–30). Paired-pulse depression (PPD) was observed at short interpulse intervals (IPIs) (Fig. 2*E*), and recovery from depression could be fit with two exponential components with time constants designated τ_{fast} and τ_{slow}. At 20 °C, τ_{fast} and τ_{slow} were 0.07 and 2.1 s, respectively (Fig. 2*F*). These values are comparable with those of two primary recovery components reported for PPD of cerebellar climbing fiber-purkinje cell (CF-PC) synapses at 24 °C (τ_{fast} and τ_{int} were 0.10 and 3.2 s, respectively) (2). Increasing the temperature to 33 °C decreased τ_{fast} and τ_{slow} to 0.04 and 1.5 s, respectively, as observed for CF-PC synapses (respective τ_{fast} and τ_{int} values were 0.04 and 1.2 s at 34 °C). The faster component of recovery in PPD, which is thought to reflect calcium-dependent refilling of the release-ready synaptic vesicle pool (2), is predominant in PPD at adult DLM neuromuscular synapses (Fig. 2 *F* and *G*), and appears to have an important role in maintaining neurotransmitter release. Finally, the size of the release-ready vesicle pool relative to the total vesicle pool, as well as the release probability, were estimated from cumulative EPSC amplitude plots (Fig. S2). The release-ready pool at DLM neuromuscular synapses represents ≈1% of the total vesicle pool as reported for other synapses (3), and the release probability is ≈0.3 under physiological conditions at 33 °C. These findings reveal conserved properties of

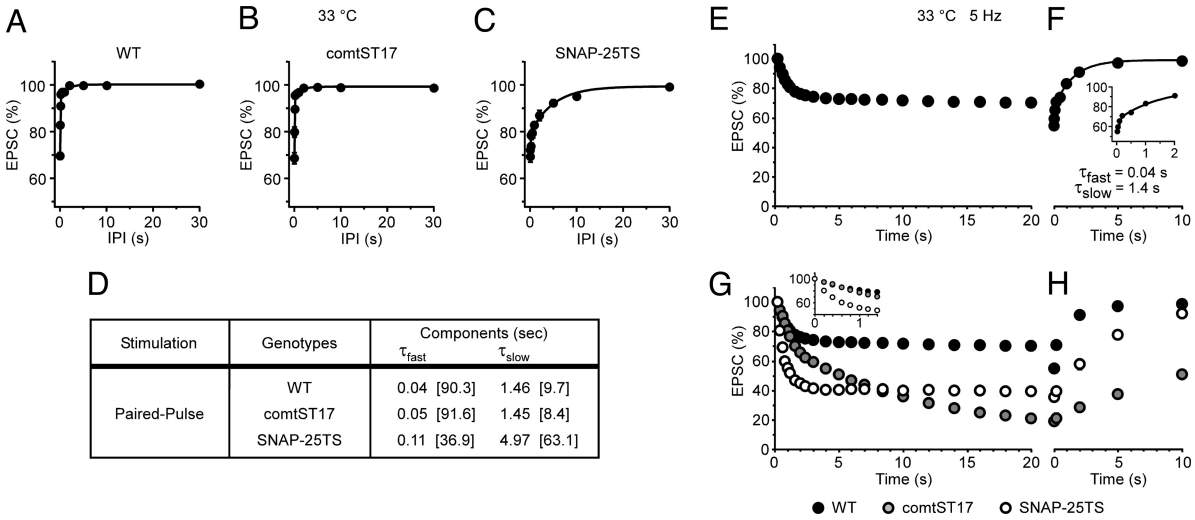

D

Stimulation	Genotypes	Components (sec) τ_{fast}	τ_{slow}
Paired-Pulse	WT	0.04 [90.3]	1.46 [9.7]
	comtST17	0.05 [91.6]	1.45 [8.4]
	SNAP-25TS	0.11 [36.9]	4.97 [63.1]

Fig. 3. Contributions of NSF and SNAP-25 to the properties of short-term synaptic depression. (*A–D*) SNAP-25 is a determinant of recovery in PPD. Time course of recovery in PPD at 33 °C in WT (*A;* as shown in Fig. 2*G*), *comatose*^{ST17} ($n = 4–7$) (*B*), and *SNAP-25*^{TS} ($n = 4–6$) (*C*) were fit with two exponential components (solid lines). (*D*) Summary of recovery components obtained from experiments shown in *A–C*. The amplitude of each component (%) is shown in brackets. Both fast and slow recovery components were preserved in *comatose*^{ST17} and disrupted in *SNAP-25*^{TS}. (*E–H*) Roles for NSF and SNAP-25 in determining short-term depression and recovery. (*E*) Train stimulation (5 Hz) of WT DLM neuromuscular synapses at 33 °C produced short-term depression followed by recovery after the train. Peak EPSC amplitudes were normalized and plotted as a function of time ($n = 43$). The 0 time point is the beginning of the stimulus train. (*F*) Recovery from the depression in WT at specific time intervals after 5-Hz stimulation (100 pulses) ($n = 4–5$). The 0 time point is the end of the stimulus train. (*Inset*) Recovery at shorter intervals of 25, 50, 100, 200, 500, 1,000, and 2,000 ms. Note that EPSC amplitudes at intervals <200 ms were smaller than the steady-state value at 5 Hz, consistent with a role for fast recovery in sustaining the EPSC amplitude. The time course of recovery was fit with two exponential components (solid line) with $\tau_{fast} = 0.04$ s (41%) and $\tau_{slow} = 1.45$ s (59%). (*G*) Short-term synaptic depression during 5-Hz stimulation (100 pulses) in *comatose*^{ST17} ($n = 20$) and *SNAP-25*^{TS}($n = 22$). (*Inset*) The initial time course of depression in *comatose*^{ST17} closely resembled that of WT, whereas the fifth EPSC amplitude in *comatose*^{ST17} was significantly different from WT ($P = 0.011$). In contrast, *SNAP-25*^{TS} exhibited immediate enhancement of synaptic depression such that the second EPSC amplitude in *SNAP-25*^{TS} was significantly smaller than that in WT ($P = 3.2 \times 10^{-19}$). (*H*) Recovery from short-term depression after 5-Hz stimulation (100 pulses) in *comatose*^{ST17} ($n = 4$) and *SNAP-25*^{TS} ($n = 4–6$). Single exponential fits of recovery in *comatose*^{ST17} and *SNAP-25*^{TS} produced time constants of $\tau = 9.8$ and 4.7 s, respectively. Because both mutants lack fast recovery after train stimulation, no increase in depression is observed at the earliest (25 ms) recovery time point.

short-term synaptic depression at adult neuromuscular synapses of *Drosophila* and establish a model for genetic analysis of their molecular determinants.

Contributions of NSF and SNAP-25 to the Properties of Short-Term Synaptic Depression. PP and train stimulation paradigms were used to examine short-term depression and recovery from depression in the *comatose* (NSF) and *SNAP-25*^{TS} mutants. Notably, the two mutants have distinct phenotypes with respect to recovery in PPD. At 33 °C, *comatose* (NSF) synapses exhibit a two-component recovery time course indistinguishable from that of WT (Fig. 3 *A*, *B*, and *D*), suggesting that the activity-dependent synaptic phenotype in *comatose* (NSF) requires sustained stimulation. In contrast, *SNAP-25*^{TS} disrupted the fast component of recovery in PPD, which was greatly diminished in weight and exhibited a slower time constant (Fig. 3 *C* and *D*). Moreover, both the weight and time constant of the slow recovery component were markedly increased. Thus, fast and slow components of recovery in PPD are SNAP-25-dependent and do not exhibit an immediate requirement for NSF function.

The influence of synaptic activity on the *comatose* (NSF) and *SNAP-25*^{TS} mutant phenotypes was further investigated by examining short-term depression elicited by 5-Hz train stimulation (100 pulses), as well as recovery from depression. This stimulation frequency was used for simplicity, because it did not produce evident facilitation as observed at 20 and 40 Hz (Fig. 2*B*). After 5-Hz stimulation at 33 °C, WT DLM neuromuscular synapses exhibited two components of recovery similar to those observed in PP experiments, with τ_{fast} and τ_{slow} values of 0.04 and 1.4 s, respectively (Fig. 3 *E* and *F*). Interestingly, the τ_{fast} component was not predominant as observed in PP experiments, but rather, the τ_{fast} and τ_{slow} components had similar weights. Both *comatose* (NSF) and *SNAP-25*^{TS} exhibited marked activity-dependent reduction in EPSC amplitude with respect to WT (Fig. 3*G*). In *comatose* (NSF), the EPSC amplitude declined progressively over 100 stimuli to 21.0 ± 0.93% ($n = 20$) of the first amplitude. As shown in Fig. 3*G* *Inset*, the initial time course of depression closely resembled that of WT over the first five stimuli (1 s). This delay in onset of the *comatose* (NSF) phenotype is consistent with preservation of the τ_{fast} component of recovery in PPD. In contrast to *comatose* (NSF), *SNAP-25*^{TS} synapses exhibited immediate enhancement of synaptic depression to a steady-state EPSC amplitude of 39.5 ± 0.82% ($n = 22$) with respect to the first amplitude (Fig. 3*G* and *Inset*). This rapid onset of the *SNAP-25*^{TS} phenotype is consistent with loss of the τ_{fast} component of recovery in PPD. Finally, recovery from depression after 5-Hz stimulation was slowed in both *comatose* (NSF) and *SNAP-25*^{TS}, and could be fit with a single exponential. Notably, recovery in *SNAP-25*^{TS} exhibited a similar time constant ($\tau = 4.7$ s) to the slow component in PP experiments. The marked slowing of recovery in *comatose* (NSF) ($\tau = 9.8$ s) after train stimulation contrasts the WT recovery in PPD, and suggests progressive disruption of synaptic function during the stimulus train (see *Discussion*).

An In Vivo Role for SNAP-25 in Refilling the Release-Ready Pool of Synaptic Vesicles. To further explore loss of fast recovery from short-term depression in *SNAP-25*^{TS}, a possible function for SNAP-25 in rapid refilling of the release-ready synaptic vesicle pool was investigated. Such a role would be consistent with elegant work in adrenal chromaffin cells, demonstrating that SNAP-25 mutations within the N-terminal portion of the SNARE four helix bundle selectively disrupts vesicle priming (13) (see *Discussion*), as well as with changes in release-ready pool size associated with different SNAP-25 variants in cultured neurons (31).

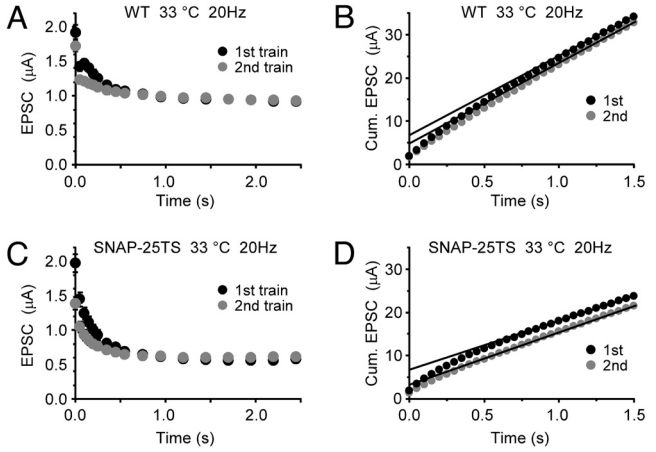

Fig. 4. Slow recovery of the release-ready vesicle pool in *SNAP-25^{TS}*. (*A* and *B*) WT peak EPSC amplitudes at 33 °C (*A*) and the corresponding cumulative (Cum.) amplitude (*B*) during paired 20-Hz stimulation trains (100 pulses) separated by a 2-s intertrain interval ($n = 5$). The first EPSC amplitude of the second train was reduced to 89.8 ± 0.70% with respect to the first amplitude of the first train. Solid lines in *B* represent back-extrapolated linear fits obtained from the cumulative amplitude data between 2.0 to 2.5 s. Release-ready pool sizes estimated from the Y intercepts (time 0) were 6.83 ± 0.49 μA for the first train, and 4.87 ± 0.31 μA for the second train, indicating a 71.6 ± 1.88% replenishment of the release-ready pool in WT. (*C* and *D*) Studies analogous to *A* and *B* in *SNAP-25^{TS}* ($n = 6$). The first EPSC amplitude of the second train was 70.5 ± 1.16% with respect to that of the first train. Release-ready pool size estimates for the first and second trains were 6.75 ± 0.56 and 3.36 ± 0.32 μA, respectively, indicating a 49.8 ± 2.35% replenishment of the release-ready pool. Percentage replenishment was significantly reduced in *SNAP-25^{TS}* with respect to WT ($P = 0.0001$).

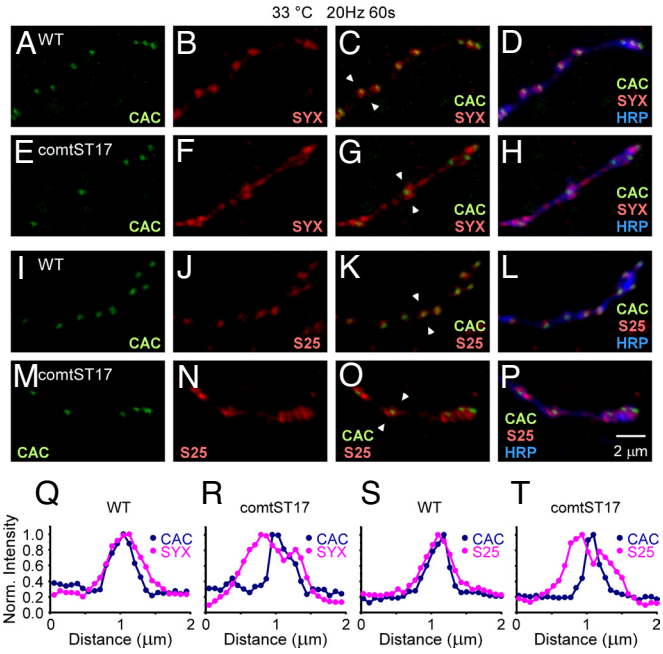

Fig. 5. t-SNARE redistribution at *comatose* (NSF) DLM neuromuscular synapses. (*A–P*) Distribution of endogenous SYNTAXIN (SYX) (*A–H*) and SNAP-25 (S25) (*I–P*) at adult DLM neuromuscular synapses with respect to active zone (CAC1-EGFP; CAC) and plasma membrane (anti-HRP) markers. In WT after 20-Hz stimulation at 33 °C (1,200 pulses), both SYNTAXIN and SNAP-25 remained associated with active zones (*A–D*, *I–L*, *Q*, and *S*). However, after stimulation in *comatose^{ST17}* at 33 °C, t-SNAREs were redistributed away from the active zone (*E–H*, *M–P*, *R*, and *T*). Each pair of white arrowheads (*C*, *G*, *K*, and *O*) designates a line of pixels whose intensities were normalized to the maximum pixel intensity and plotted as a function of distance in *Q–T*. All images represent maximum projections of two optical sections.

First, low release probability conditions were used to examine whether the *SNAP-25^{TS}* phenotype is release-dependent as predicted for a defect in refilling the release-ready pool. WT synapses in 0.2 mM extracellular calcium exhibited modest PP facilitation rather than depression (Fig. S3 *a* and *b*). At 33 °C, PP stimulation with an IPI of 10 ms produced a PP ratio (R) ($EPSC_2/EPSC_1$) of 1.12 ± 0.02 ($n = 4$). Similarly, the corresponding ratio in *SNAP-25^{TS}* under the same conditions was 1.13 ± 0.03 ($n = 4$). These findings indicate that *SNAP-25^{TS}* does not alter basic calcium-dependent properties of neurotransmitter release such as synaptic facilitation and calcium sensitivity. Rather, they suggest a release-dependent role for SNAP-25.

Further investigation of a possible function for SNAP-25 in refilling the release-ready synaptic vesicle pool involved back extrapolation of cumulative EPSC amplitude plots to obtain estimates of initial pool size (32). DLM neuromuscular synapses were stimulated with two consecutive 20-Hz stimulus trains separated by an intertrain interval of 2 s. Recovery of the release-ready pool was assessed by comparing initial pool size estimates for the first and second train. This approach is possible in *SNAP-25^{TS}* because the marked activity-dependent decline in EPSC amplitude is followed by a steady-state level of depression. In the case of WT synapses stimulated at 33 °C, the first stimulation train produced an initial release-ready pool size estimate of 6.8 ± 0.49 μA ($n = 5$) (Fig. 4 *A* and *B*), and the pool recovered to 71.6 ± 1.9% ($n = 5$) of this initial value during the intertrain interval. Notably, *SNAP-25^{TS}* exhibited a WT initial pool size for the first stimulation train (6.8 ± 0.56 μA; $n = 6$), but recovered to only 49.8 ± 2.4% ($n = 6$) during the intertrain interval (Fig. 4 *C* and *D*). These observations reveal a role for SNAP-25 in refilling the release-ready synaptic vesicle pool and identify this mechanism as an important, and likely conserved, molecular determinant of short-term synaptic depression.

Role for NSF in Maintaining Active Zone t-SNAREs During Synaptic Activity. Preservation of WT PPD in *comatose* (NSF) and the delayed onset of the synaptic phenotype during train stimulation suggest progressive disruption of synaptic function during sustained activity. Given the established role of NSF in disassembling SNARE complexes (12, 33), one possible mechanism is the progressive depletion of free SNARE proteins available for vesicle priming and fusion. This possibility was investigated by examining the distribution of endogenous SNARE proteins at neurotransmitter release sites (active zones) of DLM neuromuscular synapses. To detect changes in SNARE protein distribution, these experiments were carried out under conditions of sustained high-frequency stimulation (20 Hz; 1,200 pulses), producing a severe activity-dependent reduction of EPSC amplitudes in *comatose* (NSF) relative to WT (Fig. S4). This intensive stimulation paradigm produced a similarly strong *comatose* (NSF) synaptic phenotype at 20 °C (see *SI Methods*).

Because the plasma membrane t-SNAREs, SYNTAXIN and SNAP-25, may be limiting for formation of new SNARE complexes at active zones, the distributions of these proteins were determined relative to an active zone marker, CAC1-EGFP (34). Notably, both endogenous SYNTAXIN and SNAP-25 were concentrated at active zone regions of unstimulated WT and *comatose* (NSF) synapses maintained at 33 °C (Fig. S5), and WT synapses retained these distributions after stimulation (Fig. 5 *A–D* and *I–L*). In contrast, stimulated *comatose* (NSF) synapses exhibited a clear redistribution of both t-SNARE proteins away from the active zone (Fig. 5 *A–H* and *M–P*). Whereas intensity profiles of stimulated WT synapses show alignment of peak intensities for CAC1-EGFP, SYNTAXIN and SNAP-25 (Fig. 5 *Q* and *S*), *comatose* (NSF) synapses exhibited a relative spreading of the t-SNARE signal and a depression in intensity which aligned with the CAC1-EGFP peak (Fig. 5 *R* and *T*). In contrast to *comatose* (NSF), *SNAP-25^{TS}* did not exhibit redistribution of t-SNAREs under the same conditions (Fig.

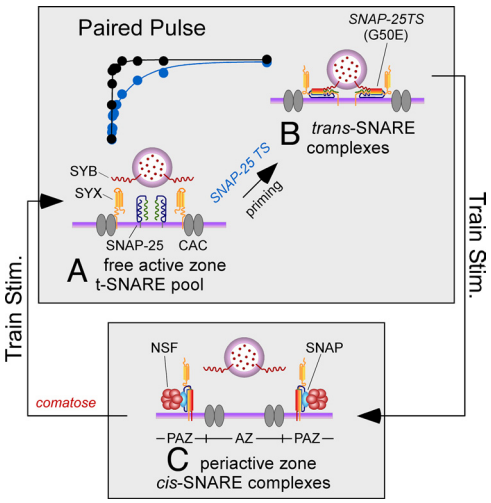

Fig. 6. Working model of SNARE protein cycling during synaptic activity. In this model, recovery in PPD depends on a limited pool of free active zone t-SNAREs (*A*), which is sufficient to support formation of *trans*-SNARE complexes (*B*) and refilling of the release-ready vesicle pool. This priming process is impaired in the *SNAP-25^{TS}* mutant (blue recovery data) with respect to WT (black recovery data). The location of the *SNAP-25^{TS}* mutation within the N-terminal region of the SNARE four helix bundle (*B*) is consistent with a zippering model of SNARE complex function. On train stimulation, *cis*-SNARE complexes (*C*) accumulate in the periactive zone (PAZ), resulting in depletion of the free t-SNARE pool at the active zone (AZ). Disassembly of *cis*-SNARE complexes by NSF and SNAP restores active zone t-SNARES for subsequent vesicle priming and fusion events. This aspect of synaptic vesicle priming is impaired in *comatose*. SYB: the v-SNARE protein, SYNAPTOBREVIN; SYX: the t-SNARE protein, SYNTAXIN; CAC, presynaptic voltage-gated calcium channel. Synaptic protein representations were modeled after those reported previously (11).

S6). Thus, redistribution of t-SNAREs away from the active zone was observed only at stimulated *comatose* (NSF) synapses. These observations suggest that NSF disassembly of plasma membrane SNARE complexes in regions adjacent to active zones (periactive zones) maintains a population of free active zone t-SNAREs. Progressive loss of this t-SNARE pool may be responsible for the *comatose* (NSF) synaptic phenotype.

Discussion

The present study further defines the in vivo roles of NSF and SNAP-25 in synaptic vesicle trafficking and their contributions to conserved properties of short-term synaptic depression. We have also gained insight into the spatial organization of activity-dependent SNARE protein cycling with respect to active zones. Our findings support a model incorporating in vivo molecular mechanisms of synaptic vesicle priming as important determinants of short-term depression and maintenance of neurotransmitter release during synaptic activity. These priming mechanisms include a direct role for SNAP-25 and an indirect contribution involving NSF-dependent replenishment of active zone free t-SNAREs for subsequent vesicle priming and fusion (Fig. 6).

In Vivo Function for SNAP-25 in Synaptic Vesicle Priming and Short-Term Depression. Our findings reveal a role for SNAP-25 in determining the properties of recovery from short-term depression (Figs. 3 and 6). An underlying function for SNAP-25 in synaptic vesicle priming was inferred from the following aspects of the *SNAP-25^{TS}* synaptic phenotype: (*i*) activity dependence as indicated by a WT initial EPSC amplitude and release-ready synaptic vesicle pool size, (*ii*) preservation of the WT EPSC waveform, (*iii*) loss of fast recovery in PPD, which is associated with fast refilling of the release-ready pool (2, 9) and exhibits a time course comparable with that of synaptic vesicle priming (35), (*iv*) dependence on previous synaptic vesicle fusion, and (*v*) slowed refilling of the release-ready vesicle pool. Thus, although SNAP-25 is required for evoked synaptic vesicle fusion (36), the *SNAP-25^{TS}* mutation can selectively affect synaptic vesicle priming. This finding is consistent with systematic structure-function analysis of SNAP-25 in adrenal chromaffin cells, which provided strong support for the zippering model of SNARE function (13). In this model, vesicle priming involves initial assembly at the N-terminal end of the SNARE four helix bundle to form a loose *trans*-SNARE complex. Final assembly of its C-terminal end, which may be triggered by calcium influx, is critical for vesicle fusion. Notably, the *SNAP-25^{TS}* mutation is positioned within the N-terminal region of the four helix bundle (Fig. 6*B*), consistent with a TS impairment of *trans*-SNARE complex formation associated with synaptic vesicle priming. Previous studies of *SNAP-25^{TS}* indicate that synaptic vesicle docking at active zones is not disrupted at larval neuromuscular synapses, and that in vivo levels of SDS-resistant (likely *cis*) SNARE complexes are not altered in this mutant (22). Finally, it will be of great interest to further investigate the relationship of SNAP-25-dependent mechanisms underlying fast and slow components of recovery. These components are thought to involve calcium-dependent regulation (2, 37, 38) of kinetically distinct synaptic vesicle pools exhibiting different release probabilities (5, 6, 8, 39–41).

In Vivo Function for NSF in Maintaining Active Zone t-SNAREs During Synaptic Activity. The close resemblance of *comatose* (NSF) and WT synapses with respect to the initial EPSC amplitude and PPD suggests *comatose* (NSF) initially exhibits a WT release-ready vesicle pool and release probability. The strictly activity-dependent reduction in neurotransmitter release observed in *comatose* (NSF) requires a brief period of synaptic activity as indicated by delayed onset of the synaptic phenotype during train stimulation (Fig. 3*G*). The underlying mechanism appears to involve activity-dependent redistribution of plasma membrane t-SNAREs away from the active zone (Fig. 5). Together with systematic biochemical studies of *comatose* (NSF) demonstrating TS accumulation of (SDS-resistant) ternary SNARE complexes on the plasma membrane (21), these findings suggest that SNAREs accumulate in plasma membrane *cis*-SNARE complexes that are not retained within the active zone (Fig. 6). NSF disassembly of post-fusion plasma membrane *cis*-SNARE complexes has been directly demonstrated in studies of yeast exocytosis and the underlying heterotypic fusion of secretory vesicles with the plasma membrane (42). Previous and present efforts to address this issue at *Drosophila* synapses, including analysis of v-SNARE distribution in the presynaptic plasma membrane (Fig. S7), are described in *SI Methods*. Finally, an alternative view of NSF function favoring prefusion disassembly of SNARE complexes was reported in a study employing caged NSF peptides to acutely disrupt NSF function at the squid giant synapse (43). However, the activity-dependent effects of the peptide on EPSC amplitude are largely consistent with the working model presented here, in which the timing of the NSF requirement is not constrained by the total vesicle cycling time (43). Although the NSF peptide was also found to slow EPSC rise and decay times, no analogous effects were observed in the present study (Fig. 1*E*).

Adult DLM Neuromuscular Synapse. The adult DLM neuromuscular synapse has had an important role in analysis of TS mutations in *comatose* (NSF) (19, 20), the presynaptic calcium channel α1 subunit gene, *cacophony* (34, 44–46), and the DYNAMIN gene, *shibire* (47–49). This work has revealed that several functional characteristics of adult neuromuscular synapses are distinct from those that we and others described previously in the larva (Fig. S8) (50, 51). In the present study, comparison of glutamatergic DLM neuromuscular synapses and cerebellar CF-PC synapses revealed a surprising degree of conservation in the detailed properties of synaptic function. These synapses exhibit morphological similarities

as well, including extensive branching of axons and spatial isolation of active zones (34, 52, 53). Initial characterization of short-term depression at CF-PC synapses has been followed by a series of studies progressively defining the underlying factors in greater detail (7, 9, 10). The present study provides a basis for analysis of DLM neuromuscular synapses to characterize analogous factors and their molecular determinants. Finally, the results reported here complement previous (49) and ongoing studies at DLM neuromuscular synapses of the DYNAMIN TS mutant, *shibire*, which exhibits a rapid enhancement of short-term depression as observed in *SNAP-25^{TS}*. Such similarities may reflect interactions of the in vivo molecular mechanisms governing synaptic vesicle endocytosis and exocytosis.

Materials and Methods

***Drosophila* Strains.** The previously characterized *SNAP-25^{TS}* and *SNAP-25^{124}* mutants were generously provided by David Deitcher (Cornell University, Ithaca, NY). WT flies were *Canton-S*. The *comatose^{ST17}*, *UAS-cac1-EGFP*, *UAS-dNSF1-FLAG*, *UAS-tdTomato-SNAP-25*, *Appl-GAL4*, *Appl-GAL4 comatose^{ST17}*, *elav-GAL4 Appl-GAL4 l(1)L13^{HC129}*, and *elav-GAL4 Appl-GAL4 l(1)L13^{HC129} comatose^{ST17}* strains were from our laboratory collection. Stocks and crosses were cultured on conventional medium at 20 °C.

Synaptic Electrophysiology. EPSCs were recorded at DLM neuromuscular synapses of 3- to 5-day-old adults essentially as described (19) with modifications. EPSCs were recorded at a holding potential of −20 mV, which optimized the recording conditions and did not alter any previously characterized DLM synaptic phenotypes. Before initiating EPSC recordings, the membrane potential was clamped to −20 mV for ≈10 min at 20 °C. For detailed information, see *SI Methods*.

Immunocytochemistry and Confocal Microscopy. Immunocytochemistry procedures were essentially the same as those described previously (34). For detailed information, see *SI Methods*.

ACKNOWLEDGMENTS. Drs. David Deitcher (Cornell University, Ithaca, NY), Erich Buchner (Univesitaet Würzburg, Würzberg, Germany) and Nicholas Harden (Simon Fraser University, Burnaby, Canada) generously provided materials for these studies. Huaru Yan contributed exceptional technical support. R.W.O. would like to thank Drs. J. J. Singer and J. V. Walsh, Jr., whose guidance and support helped to make this work possible. This work was funded by the National Science Foundation and the National Institutes of Health.

1. Zucker RS, Regehr WG (2002) Short-term synaptic plasticity. *Annu Rev Physiol* 64:355–405.
2. Dittman JS, Regehr WG (1998) Calcium dependence and recovery kinetics of presynaptic depression at the climbing fiber to Purkinje cell synapse. *J Neurosci* 18:6147–6162.
3. Rizzoli SO, Betz WJ (2005) Synaptic vesicle pools. *Nat Rev Neurosci* 6:57–69.
4. Schneggenburger R, Sakaba T, Neher E (2002) Vesicle pools and short-term synaptic depression: Lessons from a large synapse. *Trends Neurosci* 25:206–212.
5. Hosoi N, Sakaba T, Neher E (2007) Quantitative analysis of calcium-dependent vesicle recruitment and its functional role at the calyx of Held synapse. *J Neurosci* 27:14286–14298.
6. Sakaba T, Neher E (2001) Calmodulin mediates rapid recruitment of fast-releasing synaptic vesicles at a calyx-type synapse. *Neuron* 32:1119–1131.
7. Foster KA, Regehr WG (2004) Variance-mean analysis in the presence of a rapid antagonist indicates vesicle depletion underlies depression at the climbing fiber synapse. *Neuron* 43:119–131.
8. Neher E, Sakaba T (2008) Multiple roles of calcium ions in the regulation of neurotransmitter release. *Neuron* 59:861–872.
9. Foster KA, Kreitzer AC, Regehr WG (2002) Interaction of postsynaptic receptor saturation with presynaptic mechanisms produces a reliable synapse. *Neuron* 36:1115–1126.
10. Harrison J, Jahr CE (2003) Receptor occupancy limits synaptic depression at climbing fiber synapses. *J Neurosci* 15:377–383.
11. Rizo J, Südhof TC (2002) SNAREs and Munc18 in synaptic vesicle fusion. *Nat Rev Neurosci* 3:641–653.
12. Söllner TH (2003) Regulated exocytosis and SNARE function. *Mol Membr Biol* 20:209–220.
13. Sørensen JB, et al. (2006) Sequential N- to C-terminal SNARE complex assembly drives priming and fusion of secretory vesicles. *EMBO J* 25:955–966.
14. Hanson PI, Heuser JE, Jahn R (1997) Neurotransmitter release - four years of SNARE complexes. *Curr Opin Cell Biol* 7:310–315.
15. Hua SY, Charlton MP (1999) Activity-dependent changes in partial VAMP complexes during neurotransmitter release. *Nat Neurosci* 2:1078–1083.
16. Siddiqi O, Benzer S (1976) Neurophysiological defects in temperature-sensitive paralytic mutants of *Drosophila melanogaster*. *Proc Natl Acad Sci USA* 73:3253–3257.
17. Pallanck L, Ordway RW, Ganetzky B (1995) A *Drosophila* NSF mutant. *Nature* 376:25.
18. Ordway RW, Pallanck L, Ganetzky B (1994) Neurally expressed *Drosophila* genes encoding homologs of the NSF and SNAP secretory proteins. *Proc Natl Acad Sci USA* 91:5715–5719.
19. Kawasaki F, Mattiuz AM, Ordway RW (1998) Synaptic physiology and ultrastructure in *comatose* mutants define an *in vivo* role for NSF in neurotransmitter release. *J Neurosci* 18:10241–10249.
20. Kawasaki F, Ordway RW (1999) The *Drosophila* NSF protein, dNSF1, plays a similar role at neuromuscular and some central synapses. *J Neurophysiol* 82:123–130.
21. Tolar LA, Pallanck L (1998) NSF function in neurotransmitter release involves rearrangement of the SNARE complex downstream of synaptic vesicle docking. *J Neurosci* 18:10250–10256.
22. Rao SS, et al. (2001) Two distinct effects on neurotransmission in a temperature-sensitive SNAP-25 mutant. *EMBO J* 20:6761–6771.
23. Matthies HJ, Broadie K (2003) Techniques to dissect cellular and subcellular function in the *Drosophila* nervous system. *Method Cell Biol* 71:195–265.
24. Pallanck L, et al. (1995) Distinct roles for *N*-ethylmaleimide-sensitive fusion protein (NSF) suggested by the identification of a second *Drosophila* NSF homolog. *J Biol Chem* 270:18742–18744.
25. Boulianne G, Trimble WS (1995) Identification of a second homolog of *N*-ethylmaleimide-sensitive fusion protein that is expressed in the nervous system and secretory tissues of *Drosophila*. *Proc Natl Acad Sci USA* 92:7095–7099.
26. Weis S, Schneggenburger R, Neher E (1999) Properties of a model of Ca(++)-dependent vesicle pool dynamics and short term synaptic depression. *Biophys J* 77:2418–2429.
27. Betz WJ (1970) Depression of transmitter release at the neuromuscular junction of the frog. *J Physiol* 206:629–644.
28. Richards DA, Guatimosim C, Rizzoli SO, Betz WJ (2003) Synaptic vesicle pools at the frog neuromuscular junction. *Neuron* 39:529–541.
29. Dobrunz LE, Stevens CF (1997) Heterogeneity of release probability, facilitation, and depletion at central synapses. *Neuron* 18:995–1008.
30. Parker D (1995) Depression of synaptic connections between identified motor neurons in the locust. *J Neurophysiol* 74:529–538.
31. Delgado-Martínez I, Nehring RB, Sørensen JB (2007) Differential abilities of SNAP-25 homologs to support neuronal function. *J Neurosci* 27:9380–9391.
32. Schneggenburger R, Meyer AC, Neher E (1999) Released fraction and total size of a pool of immediately available transmitter quanta at a calyx synapse. *Neuron* 23:399–409.
33. Söllner T, et al. (1993) SNAP receptors implicated in vesicle targeting and fusion. *Nature* 362:318–324.
34. Kawasaki F, Zou B, Xu X, Ordway RW (2004) Active zone localization of presynaptic calcium channels encoded by the *cacophony*. *J Neurosci* 24:282–285.
35. Zenisek D, Steyer JA, Almers W (2000) Transport, capture and exocytosis of single synaptic vesicles at active zones. *Nature* 406:849–854.
36. Washbourne P, et al. (2002) Genetic ablation of the t-SNARE SNAP-25 distinguishes mechanisms of neuroexocytosis. *Nat Neurosci* 5:19–26.
37. Wang L-Y, Kaczmarek LK (1998) High-frequency firing helps replenish the readily releasable pool of synaptic vesicles. *Nature* 394:384–388.
38. Stevens CF, Wesseling JF (1998) Activity-dependent modulation of the rate at which synaptic vesicles become available to undergo exocytosis. *Neuron* 21:415–424.
39. Wu LG, Borst JG (1999) The reduced release probability of releasable vesicles during recovery from short-term synaptic depression. *Neuron* 23:821–832.
40. Wadel K, Neher E, Sakaba T (2007) The coupling between synaptic vesicles and Ca^{2+} channels determines fast neurotransmitter release. *Neuron* 53:563–575.
41. Wölfel M, Lou X, Schneggenburger R (2007) A mechanism intrinsic to the vesicle fusion machinery determines fast and slow transmitter release at a large CNS synapse. *J Neurosci* 27:3198–3210.
42. Grote E, Carr CM, Novick PJ (2000) Ordering the final events in yeast exocytosis. *J Cell Biol* 151:439–451.
43. Kuner T, et al. (2008) Photolysis of a caged peptide reveals rapid action of N-ethylmaleimide sensitive factor before neurotransmitter release. *Proc Natl Acad Sci USA* 105:347–352.
44. Kawasaki F, Felling R, Ordway RW (2000) A temperature-sensitive paralytic mutant defines a primary synaptic calcium channel in *Drosophila*. *J Neurosci* 20:4885–4889.
45. Kawasaki F, Collins SC, Ordway RW (2002) Synaptic calcium channel function in *Drosophila*: Analysis and transformation rescue of temperature-sensitive paralytic and lethal mutations of *cacophony*. *J Neurosci* 22:5856–5864.
46. Brooks IM, Felling R, Kawasaki F, Ordway RW (2003) Genetic analysis of a synaptic calcium channel in *Drosophila*: Intragenic modifiers of a temperature-sensitive paralytic mutant of *cacophony*. *Genetics* 164:163–171.
47. Kosaka T, Ikeda K (1983) Possible temperature-dependent blockage of synaptic vesicle recycling induced by a single gene mutation in *Drosophila*. *J Neurobiol* 14:207–225.
48. Koenig JH, Ikeda K (1999) Contribution of active zone subpopulation of vesicles to evoked and spontaneous release. *J Neurophysiol* 81:1495–1505.
49. Kawasaki F, Hazen M, Ordway RW (2000) Fast synaptic fatigue in *shibire* mutants reveals a rapid requirement for dynamin in synaptic vesicle membrane trafficking. *Nat Neurosci* 3:859–860.
50. Mohrmann R, Matthies HJ, Woodruff EI, Broadie K (2008) Stoned B mediates sorting of integral synaptic vesicle proteins. *Neuroscience* 153:1048–1063.
51. Wu Y, Kawasaki F, Ordway RW (2005) Properties of short-term synaptic depression at larval neuromuscular synapses in wild-type and temperature-sensitive paralytic mutants of *Drosophila*. *J Neurophysiol* 93:2396–2405.
52. Hebbar S, Fernandes JJ (2004) Pruning of motor neuron branches establishes the DLM innervation pattern in Drosophila. *J Neurobiol* 60:499–516.
53. Ikeda K, Koenig JH (1988) Morphological identification of the motor neurons innervating the dorsal longitudinal flight muscle of *Drosophila melanogaster*. *J Comp Neurol* 273:436–444.